

Kinetin Riboside and Its ProTides Activate the Parkinson's Disease Associated PTEN-Induced Putative Kinase 1 (PINK1) Independent of Mitochondrial Depolarization

Laura Osgerby,^{†,‡} Yu-Chiang Lai,^{‡,§} Peter J. Thornton,[§] Joseph Amalfitano,[†] Cécile S. Le Duff,[†] Iqra Jabeen,[†] Hachemi Kadri,[§] Ageo Miccoli,^{||} James H. R. Tucker,[†] Miratul M. K. Muqit,^{*,‡,⊥} and Youcef Mehellou^{*,||}

[†]School of Chemistry, University of Birmingham, Birmingham, B15 2TT, U.K.

[‡]MRC Protein Phosphorylation and Ubiquitylation Unit, University of Dundee, Dundee DD1 5EH, U.K.

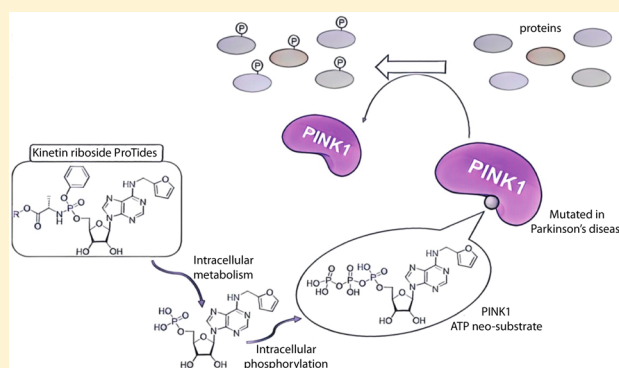
[§]School of Pharmacy, University of Birmingham, Birmingham, B15 2TT, U.K.

^{||}School of Pharmacy and Pharmaceutical Sciences, Cardiff University, Cardiff CF10 3NB, U.K.

[⊥]School of Medicine, University of Dundee, Dundee, DD1 9SY, U.K.

Supporting Information

ABSTRACT: Since loss of function mutations of PINK1 lead to early onset Parkinson's disease, there has been growing interest in the discovery of small molecules that amplify the kinase activity of PINK1. We herein report the design, synthesis, serum stability, and hydrolysis of four kinetin riboside ProTides. These ProTides, along with kinetin riboside, activated PINK1 in cells independent of mitochondrial depolarization. This highlights the potential of modified nucleosides and their phosphate prodrugs as treatments for neurodegenerative diseases.



Parkinson's disease (PD) is the second most common neurodegenerative disease in the world.¹ It affects around 130 000 people in the U.K. and over 1 million people in the U.S.¹ Considering that current PD therapies and medical interventions are limited only to addressing the symptoms of this disease² coupled with a general rise in lifespan, the rate of PD incidence in the future is likely to increase significantly. This highlights the need for new and specific PD treatments. As part of our efforts into discovering novel PD therapeutics, we focused on PINK1 (PTEN-induced kinase 1), a protein kinase mutated in some patients with early onset PD.³

PINK1 is a mitochondrial serine/threonine protein kinase that possesses a unique N-terminal mitochondrial targeting sequence, a transmembrane domain, and three insertional loops within its catalytic kinase domain.⁴ Following inner mitochondrial membrane depolarization, it becomes stabilized on the outer mitochondrial membrane (OMM) where it phosphorylates the E3 ubiquitin ligase Parkin at serine 65 (Ser65) on its N-terminal ubiquitin-like domain. Such phosphorylation activates Parkin, which is also mutated in early onset PD,⁵ leading to the ubiquitylation of a series of its substrates on the OMM that act as a signal for the degradation of mitochondria by autophagy (mitophagy).⁶

In PD, the majority of PINK1 mutations are located within its kinase domain and consequently affect its catalytic activity.^{7,8} This confirms that the kinase activity of PINK1 is critical to the prevention of neurodegeneration. This notion has been verified in *Drosophila* models of PINK1 in which kinase-inactive versions of PINK1 failed to rescue neurodegeneration compared to the wild-type gene.⁹ Hence, the activation of PINK1 emerged as a useful strategy to induce and maintain neuroprotective effects, an approach that would be useful in treating PD.

To date, reported efforts into the discovery of small molecules that activate PINK1 led to the identification of *N*⁶-furfuryladenine, termed kinetin (1, Figure 1),¹⁰ which is undergoing clinical trials for the treatment of familial dysautonomia and the prevention from skin photodamage.¹¹ In cells, pronounced activation of PINK1 by kinetin was only observed following co-incubation with the mitochondrial-depolarizing agent CCCP (carbonyl cyanide *m*-chlorophenylhydrazine),⁵ which in itself activates PINK1 in cells.¹² Studies into the mechanism by which PINK1 is activated by kinetin revealed that kinetin was converted intracellularly in four

Received: December 23, 2016

Published: March 21, 2017

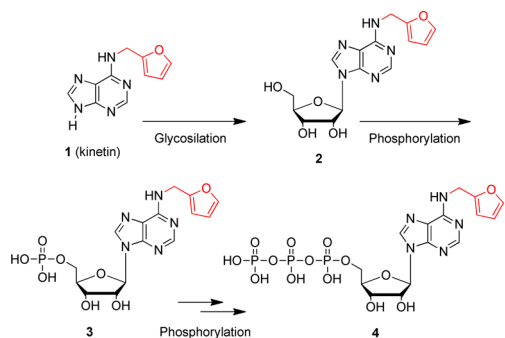


Figure 1. Chemical structure of kinetin (**1**) and its metabolism in cells to generate the active substrate kinetin riboside triphosphate (**4**).

consecutive metabolic steps to the active metabolite kinetin riboside (KR) triphosphate (**4**), which acts as a PINK1 ATP-neosubstrate (Figure 1).¹⁰

Given that the cellular activation of synthetic nucleobases and their nucleoside derivatives may be of limited efficiency as compared to natural nucleobases and nucleosides, we explored the direct use of the KR monophosphate intermediate (**3**) as an activator of PINK1 in cells would bypass two important activation steps, glycosylation and the first phosphorylation step, that kinetin must undergo consecutively. This suggests that KR monophosphate would be a more potent activator of PINK1 than kinetin. As nucleoside monophosphates often have poor *in vivo* stability and inefficient cellular uptake, we employed the ProTide prodrug technology¹³ to deliver KR monophosphate into cells. This prodrug technology has inspired the discovery of two FDA-approved (antiviral) nucleotide monophosphate and monophosphonate drugs with many more undergoing clinical trials.¹⁴

The synthesis of KR ProTides started by making kinetin riboside in a single step from 6-chloropurine riboside (**10**) as reported (Figure 2).¹⁵ This involved refluxing 6-chloropurine

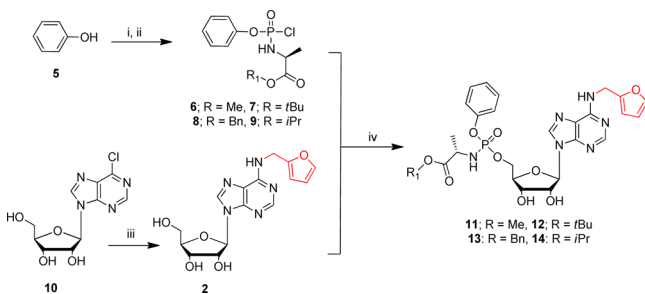


Figure 2. Synthesis of kinetin riboside and its ProTides. Reagents and conditions: (i) POCl_3 , TEA, Et_2O , -78°C ; (ii) L-alanine ester hydrochloride, TEA, DCM, -78°C ; (iii) furfurylamine, TEA, EtOH, N_2 , 77°C , (iv) $^t\text{BuMgCl}$ or NMI, DCM, N_2 , rt.

riboside with furfurylamine in ethanol in the presence of triethylamine. The pure product was subsequently coupled¹⁶ with the appropriate phosphorochloridate (**6–9**) in the presence of $^t\text{BuMgCl}$ or NMI as a base to afford the desired KR ProTides (**11–14**).

In the design of these ProTides, the amino acid of the ProTides was fixed as L-alanine, since this historically¹⁷ has given the optimum biological activity and is processed well by enzymes during the metabolism of the ProTides *in vivo*. A small selection of ester motifs was used in this study [methyl

(Me), isopropyl (^iPr), *tert*-butyl (^tBu), and benzyl (Bn)] to probe the influence of these moieties on the ProTides' biological activity.

Since these ProTides are prodrugs aimed at delivering KR monophosphate, we initially explored the hydrolysis of the phosphate masking groups to release the naked KR monophosphate. The intracellular metabolism¹⁸ of ProTides is known to be triggered by esterase enzymes, such as cathepsin A,¹⁹ which cleave off the ester motif (Figure 3). The generated

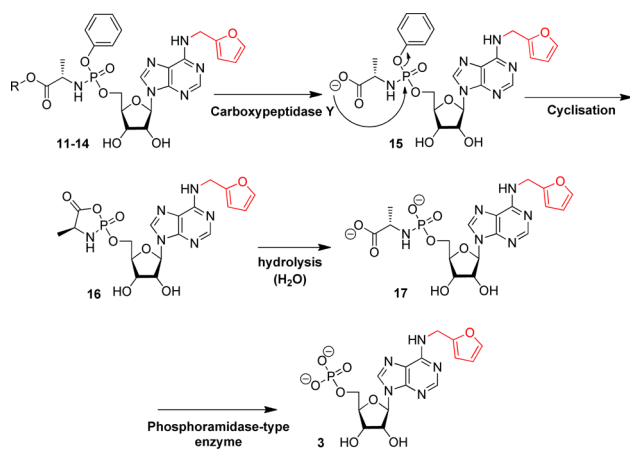


Figure 3. Postulated mechanism of *in vivo* metabolism of ProTides to release nucleoside analogue monophosphates.

carboxylate group (**15**) undergoes a nucleophilic attack on the phosphate group resulting in the loss of the phenyl group and the formation of an unstable five-membered heterocyclic ring (**16**). A water molecule subsequently attacks the phosphate group to open this ring and generate metabolite **17**. Finally, a phosphoramidase-type enzyme, e.g., Hint-1,^{20–22} hydrolyzes the P–N bond of metabolite **17** leading to the release of the KR monophosphate.

To probe the hydrolysis of KR ProTides to release KR monophosphate, we followed the hydrolysis of the KR ProTide **14** by ^{31}P NMR in the presence of recombinant cathepsin A (Figure 4A).¹⁶ We chose KR ProTide **14** as it has an L-alanine isopropyl moiety akin to the two ProTides approved for use in the clinics, e.g., sofosbuvir and tenofovir alafenamide, which both bear the same L-alanine isopropyl ester moiety.¹⁷ Before the addition of the enzyme, ProTide **14** (in acetone- d_6) showed two peaks (δ_{p} 3.58 and 3.88) corresponding to its two diastereoisomers. After ~ 15 min incubation with cathepsin A in Trizma buffer, two peaks at δ_{p} 3.7 and 4.1 appeared, which correspond to the parent ProTide diastereoisomers under the acetone- d_6 /Trizma buffer. After ~ 2 h, a new peak at δ_{p} 6.81 started appearing. This corresponds to metabolite **17** in agreement with previous reports.¹⁶ Following 12 h, almost all of ProTide **14** was converted to metabolite **17** and after 48 h incubation a new peak, δ_{p} -0.11 , appeared, a typical ^{31}P NMR shift of nucleoside monophosphates. Indeed, negative ion electrospray ionization mass spec analysis of the sample showed that this new peak had a mass of 426.1 g/mol, which matches the mass of KR monophosphate **3** (MW = 427.31 g/mol) (Supporting Information Figure S1). Although in this sample, there was no phosphoramidase-type enzyme, e.g., Hint-1, that cleaves the P–N bond of intermediate **17** to generate the monophosphate species, it appears that the P–N bond of metabolite **17** was unstable under the assay condition after >48

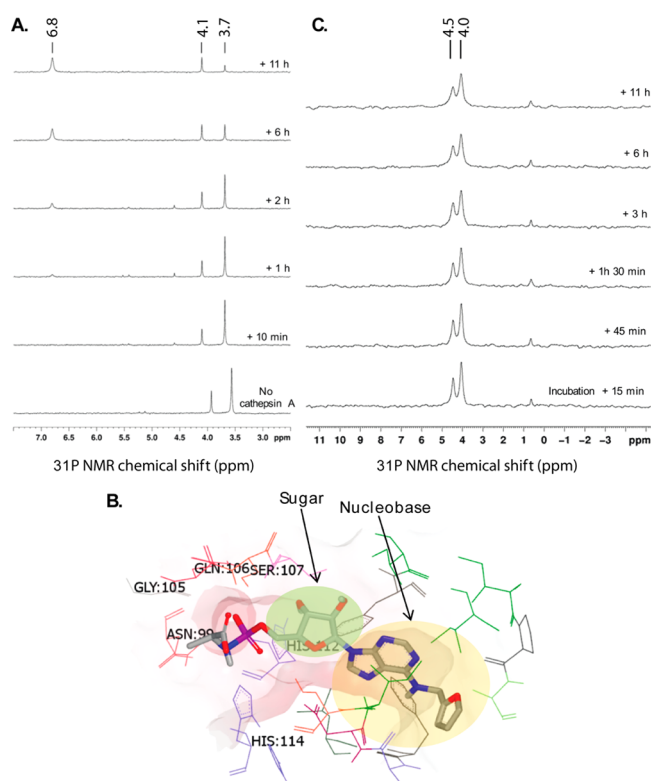


Figure 4. Metabolism and serum stability of KR ProTides. (A) ^{31}P NMR of cathepsin A mediated *in vitro* degradation of KR ProTide 14. (B) Docking of metabolite 17 into the crystal structure of Hint-1 to predict the cleavage of the P–N bond. (C) Stability of KR ProTide 14 in human serum over 12 h as monitored by ^{31}P NMR.

h of incubation. Together, the data indicated that incubation of a KR ProTide with cathepsin A triggered its hydrolysis to the major metabolite 17 with a trace of KR monophosphate.

To verify whether the kinetin riboside amidate 17 would be a good substrate for the carboxypeptidase Hint-1, which cleaves the P–N bonds of phosphoramidates,^{20–22} we performed *in silico* docking of metabolite 17 into the cocrystal structure of Hint-1 with AMP (Figure 4B). Analysis of the different predicted poses indicated that the KR nucleobase was stabilized by hydrophobic interactions with two phenylalanine residues (F19 and F41) and isoleucine (I44). Critically, the phosphate moiety was placed where the phosphate group of AMP was located while the phosphoramidate motif was positioned in a pocket that included the key amino acid residues required for the Hint-1 catalytic activity (serine 107, histidines 112 and 114). Such position suggests that metabolite 17 is likely to be processed by Hint-1 to release KR monophosphate, in agreement with previous conclusions.¹⁶

Subsequently, we examined the stability of KR ProTides in human and mouse serum *in situ*. For this, we incubated KR ProTide 14 in human (Figure 4C) or mouse serum (Supporting Information Figure S2) at 37 °C and followed the sample by ^{31}P NMR. At $t = 0$, two close ^{31}P NMR signals δ_{P} 4.0 and 4.5 ppm corresponding to the two diastereoisomers of KR ProTide 14 were present. The time-course ^{31}P NMR revealed that no new peaks appeared that may correspond to new metabolites. Indeed, following ~11 h incubation in human and mouse serum there were no changes in the ^{31}P NMR signals that correspond to the KR ProTide indicating its stability in these environments. Additionally, we studied the

stability of KR ProTides in acid environment. For this, we incubated ProTide 14 in acidic buffer, pH 1, and monitored it by ^{31}P NMR over 12 h. The data showed that the ProTide was completely stable in this acidic environment, pH 1, since the phospho peaks corresponding to ProTide 14 persisted throughout the 12 h period studied (Supporting Information Figure S3).

Once the hydrolysis and stability of KR ProTides were established, we then investigated their ability to activate PINK1 in cells. Briefly, HEK293 Flp-In TReX HEK293 cells stably expressing wild-type PINK1 were co-transfected with untagged wild type Parkin. Upon activation, PINK1 directly phosphorylates Parkin at Ser65,²³ and this phosphorylation site was used as a readout for the activity of PINK1 in cells. Initially, the cells were treated with 50 μM kinetin, KR, or KR ProTides (11–14) for 24 h (Figure 5).

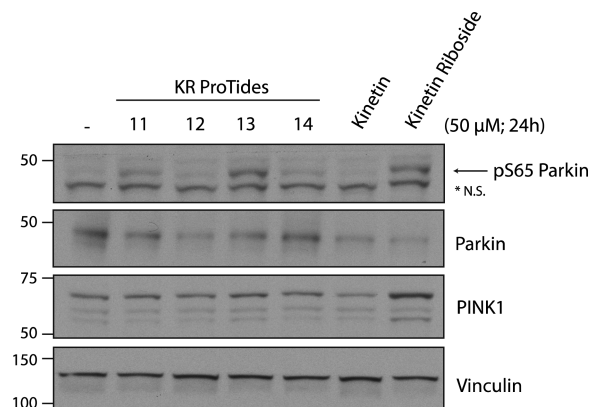


Figure 5. Activation of PINK1 by KR ProTides in cells. Flp-In TReX HEK293 cells stably expressing PINK1 were transfected with wild-type Parkin. Cells were transfected with 50 μM KR ProTides 11–14, kinetin, or kinetin riboside for 24 h. Cells were then lysed and probed with anti-phospho Ser65 Parkin (pS65 Parkin), total parkin, PINK1, and vinculin antibodies. *NS: nonspecific band.

Interestingly three out of the four KR ProTides showed activation of PINK1, as judged by Parkin Ser65 phosphorylation in the absence of CCCP treatment. KR ProTide 13 exhibited the most significant activation followed by ProTides 14 and 11. Notably, KR also showed significant activation of PINK1 while treatment with kinetin did not lead to noticeable PINK1 activation in the absence of CCCP.

The activation of PINK1 by KR ProTides indicates that the ProTides were metabolized to release KR monophosphate, which was then further phosphorylated to the active triphosphate counterpart to act as a PINK1 ATP-neosubstrate. This possibility is supported by the lack of PINK1 activation with KR ProTide 12, which has the ^tBu ester motif that is known to be poorly metabolized *in vivo* by esterases as compared to ProTides with Me, ⁱPr, and Bn esters.¹³ In fact, *in vitro* cathepsin A hydrolysis of KR ProTide 12 was very slow after a 12 h incubation with the esterase enzyme cathepsin A as ~50% of the parent ProTide remained intact (Supporting Information Figure S4) in contrast to ProTide 14, which was rapidly hydrolyzed (Figure 5). The fact that KR showed comparable PINK1 activation to KR ProTides suggests that the first phosphorylation step by which KR is converted into its monophosphate species, and which is bypassed by the ProTides, is not the rate limiting step but is its activation. This is seen with other therapeutic nucleosides such as

lamivudine and zidovudine for which the first phosphorylation step is not the rate-limiting in their activation but the second or the third phosphorylation steps.²⁴

Since the activation of PINK1 by KR and its ProTides was determined after a 24 h incubation (Figure 5), we next determined the time-dependent activation of PINK1 in cells by the most potent KR ProTide activator of PINK1, **13**. Under similar conditions, we treated cells with ProTide **13** for 3, 6, 12, 24, and 48 h (Figure 6). The data show that KR ProTide **13**

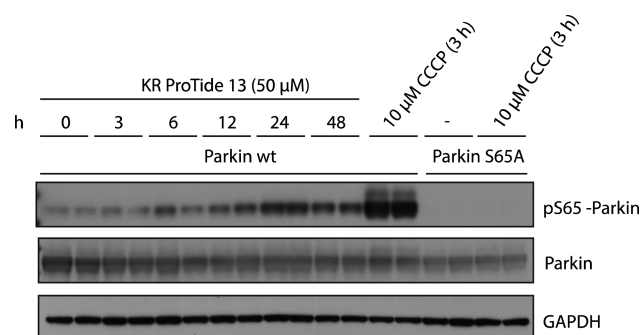


Figure 6. Time-dependent activation of PINK1 by KR ProTide **13** in cells. Flp-In TRex HEK293 cells stably expressing PINK1 were transfected with wild-type or S65A Parkin. Experiment was performed as in Figure 5.

activated PINK1 in a time-dependent manner with the most prominent activation observed after a 24 h treatment. The activation, however, was not as significant as achieved with CCCP, and no phosphorylation of Parkin was detected in cells expressing the Parkin S65A mutant as expected.

In conclusion, we herein described the first application of the powerful ProTide phosphate prodrug technology to elaborate nucleoside-based molecules that activate PINK1 in cells. Of the four KR ProTides synthesized and studied in this work, three KR ProTides showed activation of the kinase activity of PINK1 with KR ProTide **13** exhibiting the highest potency. Uniquely, this activation was independent of CCCP, a mitochondrial depolarizing agent, which has been used previously¹⁰ in identifying kinetin as an activator of PINK1. In view of the ability of these KR ProTides to activate PINK1, it may be promising to optimize these further as potential neuroprotective agents for PD. Such endeavor is supported by the favorable human and mouse serum stability profiles of these ProTides in addition to their encouraging stability in acidic environments. Notably, our approach of using the ProTide technology in developing protein kinase activators has the potential to be expanded to the discovery of ATP-neosubstrates for other protein kinases beyond PINK1 and neurodegeneration.

EXPERIMENTAL SECTION

General Information. Dichloromethane, diethyl ether, methanol, and toluene were dried in-house using a Pure Solv-MD solvent purification system. All the other solvents were used as received from commercial suppliers. All of the other reagents used in the synthesis were purchased from Sigma-Aldrich except L-alanine isopropyl ester. All reactions were carried out under an argon atmosphere. Reactions were monitored with analytical TLC on silica gel 60-F254 precoated aluminum plates and visualized under UV (254 nm) and/or with ³¹P NMR spectra. Column chromatography was performed on silica gel (35–70 μM). NMR data were recorded on a Bruker AV300, AVIII300, AV400, AVIII400, or DRX500 spectrometer in the deuterated solvents

indicated, and the spectra were calibrated on residual solvent peaks. Chemical shifts (δ) are quoted in ppm, and *J* values are quoted in Hz. In reporting spectral data, the following abbreviations were used: s (singlet), d (doublet), t (triplet), q (quartet), dd (doublet of doublets), and m (multiplet). HPLC was carried out on a DIONEX summit P580 quaternary low pressure gradient pump with a built-in vacuum degasser using a Summit UVD 170s UV/vis multichannel detector. Solvents were used as HPLC grade. Chromeleon software was used to visualize and process the obtained chromatograms. Analytical separations used a flow rate of 1 mL/min, semipreparative used a flow rate of 3 mL/min, and preparative used a flow rate of 20 mL/min. All tested compounds had a purity of ≥95% as shown by HPLC or elemental analysis (see Supporting Information).

Kinetin Riboside (2).¹⁵ Furfurylamine (0.54 mL, 6.2 mmol) and Et₃N were added dropwise to a suspension of 6-chloropurine riboside **10** (600 mg, 2.1 mmol) in EtOH (30 mL). This was refluxed for 18 h at 60 °C. The resulting yellow solution was evaporated under reduced pressure to yield the crude mixture as a cream paste. This was washed with Et₂O (3 × 25 mL) and filtered to give the product as a white crystalline solid (679 mg, 93%). ¹H NMR (400 MHz, MeOD) δ 8.26 (2H, s, H-2/H-8), 7.43 (1H, dd, *J* = 1.9, 0.9 Hz, CH₂ArO-H), 6.34 (1H, dd, *J* = 3.2, 1.8 Hz, CH₂ArO-H), 6.31 (1H, dd, *J* = 3.2, 0.9 Hz, CH₂ArO-H), 5.95 (1H, d, *J* = 6.4 Hz, 1'-H), 4.80 (2H, s, NH₂CH₂), 4.74 (1H, dd, *J* = 6.4, 5.1 Hz, 2'-H), 4.31 (1H, dd, *J* = 5.1, 2.5 Hz, 3'-H), 4.16 (1H, q, *J* = 2.5 Hz, 4'-H), 3.81 (2H, ddd, *J* = 57.3, 12.6, 2.6 Hz, 5'-H₂); ¹³C NMR (100 MHz, MeOD) 152.0 (C-8/C-2), 151.6 (CH₂ArO-C), 149.6, 147.8 (ArN-C), 142.0 (CH₂ArO-CH), 140.3 (C-8/C-2), 119.9 (ArN-C), 110.0 (CH₂ArO-CH), 106.9 (CH₂ArO-CH), 89.9 (1'-C), 86.8 (4'-C), 74.0 (2'-C), 71.3 (3'-C), 62.1 (5'-C), 36.7 (NHCH₂). MS-ESI (*m/z*): C₁₅H₁₇N₅O₅ [M + Na]⁺ 370.1.

Phenyl (Methoxy-L-alanyl)phosphorochloridate (6).¹⁶ L-Alanine methyl ester hydrochloride (400 mg, 2.9 mmol) was dissolved in anhydrous CH₂Cl₂ (20 mL) under an inert atmosphere. Following this, phenyl phosphorodichloridate (0.53 mL, 2.9 mmol) was added dropwise over 15 min. Et₃N (0.77 mL, 5.8 mmol) was then added at -78 °C, and the mixture was stirred for 30 min. The solution was then allowed to warm to room temperature over 2 h. Solvent was then removed under reduced pressure and the remaining white precipitate suspended in anhydrous Et₂O (50 mL). This was filtered and the filtrate evaporated under reduced pressure, yielding the crude product as a light brown oil. Purification via flash column chromatography gave the pure product as a colorless oil (729 mg, 91%) (eluent 7:3 EtOAc/hexane). ³¹P NMR (120 MHz, CDCl₃) δ 7.94, 7.62; ¹H NMR (400 MHz, CDCl₃) δ 7.45–7.33 (2H, m, Ar-H), 7.31–7.21 (3H, m, Ar-H), 4.62–4.52 (1H, m, N-H), 4.26–4.14 (1H, m, CHCH₃), 3.79, 3.77 (2H, 2 s, OCH₃), 1.51 (3H, dd, *J* = 7.1, 4.1 Hz, CHCH₃); ¹³C NMR (100 MHz, CDCl₃) δ 173.4 (COCH₃), 150.1 (Ar-COP), 130.3, 126.4, 121.0 (Ar-CH), 53.3 (OCH₃), 51.1 (CHCH₃), 20.9 (CHCH₃).

Phenyl (tert-Butyloxy-L-alanyl)phosphorochloridate (7).¹⁶ Prepared as described for **6** using L-alanine *tert*-butyl ester hydrochloride (400 mg, 2.20 mmol), phenyl phosphorodichloridate (0.30 mL, 2.20 mmol), and Et₃N (0.60 mL, 4.4 mmol). Product **7** was obtained as a pale yellow oil, which was used in sequential steps without further purification (803 mg, 114%). ³¹P NMR (120 MHz, CDCl₃) δ 8.26, 7.84; ¹H NMR (400 MHz, CDCl₃) δ 7.44–7.32 (2H, m, Ar-H), 7.30–7.20 (3H, m, Ar-H), 4.28 (1H, br s, NH), 4.12–3.98 (1H, m, CHCH₃), 1.56–1.34 (3H, m, CHCH₃, 9H, m, OC^tBu); ¹³C NMR (100 MHz, CDCl₃) δ 171.9 (COC^tBu), 149.9 (Ph-COP), 130.0, 126.1, 120.1 (Ph-CH), 82.9 (OC^tBu), 51.0 (CHCH₃), 28.1 (OC^tBu), 20.8 (CHCH₃).

Phenyl (Benzoyloxy-L-alanyl)phosphorochloridate (8).¹⁶ Prepared as described for **6** using L-alanine benzyl ester hydrochloride (500 mg, 2.32 mmol), phenyl phosphorodichloridate (0.35 mL, 2.32 mmol), and Et₃N (0.63 mL, 4.64 mmol). Product **8** was obtained as a pale yellow oil (505 mg, 95%). ³¹P NMR (120 MHz, CDCl₃) δ 7.85, 7.49; ¹H NMR (400 MHz, CDCl₃) δ 7.40–7.32 (m, 5H, Ph-H), 7.28–7.21 (m, 5H, Ph-H), 5.21 (2H, d, *J* = 6.1 Hz, OCH₂Ph), 4.31–4.15 (2H, 2 m, CHCH₃), 1.52 (3H, dd, *J* = 6.6, 2.4 Hz CHCH₃); ¹³C NMR (100 MHz, CDCl₃) δ 172.6 (COOCH₂Ph), 149.7 (Ph-C), 135.0 (Ph-

C), 130.0, 128.7, 128.6, 128.4, 126.0, 126.0 (Ph-CH), 67.6 (OCH₂Ph), 50.8 (CHCH₃), 20.6 (CHCH₃).

Phenyl (Isopropoxy-L-alaninyl)phosphorochloridate (9).¹⁶

Prepared as described for **6** using L-alanine isopropyl ester hydrochloride (700 mg, 4.18 mmol), phenyl phosphorodichloridate (0.62 mL, 4.18 mmol), and Et₃N (1.13 mL, 8.36 mmol). Product **9** was obtained as a yellow oil (1185 mg, 93%). ³¹P NMR (120 MHz, CDCl₃) δ 8.10, 7.80; ¹H NMR (400 MHz, CDCl₃) δ 7.46–7.32 (2H, m, Ar-H), 7.30–7.19 (3H, m, Ar-H), 5.16–5.00 (1H, m, OCHⁱPr), 4.50–4.30 (1H, m, N-H), 4.22–4.03 (1H, m, CHCH₃), 1.52–1.47 (3H, m, CHCH₃), 1.32–1.22 (6H, m, OCHⁱPr); ¹³C NMR (100 MHz, CDCl₃) δ 172.2 (COCH₃), 149.9 (Ar-COP), 130.0, 126.1, 120.7 (Ar-CH), 69.8 (OCHⁱPr), 50.8 (CHCH₃), 21.8 (2C, OCHⁱPr), 20.6 (CHCH₃).

Phenyl (Methoxy-L-alaninyl) Kinetin Riboside Phosphoramidate (11). KR 2 (200 mg, 0.60 mmol) was suspended in anhydrous THF (15 mL) under an inert atmosphere. To this, ⁴BuMgCl (0.09 mL, 0.68 mmol) was then added dropwise over 15 min. The resulting solution was stirred for 10 min, and following this, **6** (241 mg, 0.86 mmol) in anhydrous THF (1.5 mL) was then added dropwise over 10 min. The mixture was left to stir for 18 h. MeOH (2 mL) was then added to quench the reaction before solvent was removed under reduced pressure to leave the crude product as a pale yellow oil. This was purified via flash column chromatography and then preparative TLC to yield the final product as a white solid (34 mg, 10%) (eluent 3:97 to 5:95 MeOH/CH₂Cl₂). ³¹P NMR (120 MHz, MeOD) δ 3.84, 3.69; ¹H NMR (400 MHz, MeOD) δ 8.27 (1H, s, ArN-CH), 8.23, 8.20 (1H, 2 s, ArN-CH), 7.43 (1H, m, CH₂ArO-H), 7.30 (2H, t, J = 7.9 Hz, Ph-H), 7.22–7.12 (3H, m, Ph-H), 6.34 (1H, dd, J = 3.4, 1.8 Hz, CH₂ArO-H), 6.32 (1H, d, J = 2.8 Hz, CH₂ArO-H), 6.04 (1H, t, J = 5.0 Hz, 1'-H), 4.80 (2H, br s, NHCH₂), 4.70–4.60 (1H, m, 2'-H), 4.46–4.30 (3H, m, 3'-H/5'-H₂), 4.29–4.23 (1H, m, 4'-H), 3.95–3.77 (2H, 2 m, CHCH₃), 3.61 (3H, s, OCH₃), 1.30–1.27 (3H, m, CHCH₃); ¹³C NMR (100 MHz, MeOD) δ 175.5 (COOCH₃), 154.0 (ArN-CH), 153.4 (ArO-C), 152.1 (Ph-C), 150.3 (ArN-C), 143.4 (ArO-CH), 140.7 (ArN-CH), 130.7, 126.2, 121.9 (Ph-CH), 120.9 (ArN-C), 111.4, 108.2 (ArO-CH), 90.0 (1'-C), 84.4 (4'-C), 75.4 (2'-C), 71.6 (3'-C), 67.3 (5'-C), 52.7 (OCH₃), 51.4 (CHCH₃), 38.4 (NHCH₂), 20.3 (CHCH₃). HRMS-ESI (*m/z*): calcd for C₂₅H₂₉N₆O₉NaP [M + Na]⁺ 611.1631, found 611.1633. Found: C 51.2, H 5.3, N 14.2. Calcd for C₂₅H₂₉N₆O₉P: C 51.0, H 4.97, N 14.3%.

Phenyl (tert-Butyloxy-L-alaninyl) Kinetin Riboside Phosphoramidate (12). Prepared as described for compound **11** using KR 2 (200 mg, 0.60 mmol), NMI (0.22 mL, 3.00 mmol), and **7** (552 mg, 1.80 mmol). The crude product was purified via flash column chromatography to yield the final product as a white solid (52 mg, 14%) (eluent 3:97 to 5:95 MeOH/CH₂Cl₂). ³¹P NMR (120 MHz, MeOD) δ 3.91, 3.84; ¹H NMR (400 MHz, MeOD) δ 8.22 (1H, s, ArN-CH), 8.22, 8.19 (1H, 2 s, ArN-CH), 7.43 (1H, dd, J = 1.9, 0.9 Hz, CH₂ArO-H), 7.35–7.26 (2H, m, Ph-H), 7.21–7.10 (3H, m, Ph-H), 6.34 (1H, dd, J = 3.2, 1.9 Hz, CH₂ArO-H), 6.32–6.30 (1H, m, CH₂ArO-H), 6.05–6.02 (1H, m, 1'-H), 4.79 (2H, s, NHCH₂), 4.65 (1H, t, J = 5.2 Hz, 2'-H), 4.48–4.30 (3H, m, 3'-H/5'-H₂), 4.29–4.24 (1H, m, 4'-H), 3.82–3.75 (1H, m, CHCH₃), 1.39 (9H, s, ^tBu-H), 1.23 (3H, dd, J = 7.1, 1.2 Hz, CHCH₃); ¹³C NMR (100 MHz, MeOD) δ 172.9 (CO), 154.3 (ArN-C), 152.6 (ArNC-H), 151.8 (ArO-C), 150.7 (PhCOP), 148.6 (ArN-C), 142.0 (ArOC-H), 139.3 (ArNC-H), 129.4, 124.7, 120.0 (PhC-H), 119.2 (ArN-C), 110.0, 106.8 (ArOC-H), 88.6 (1'-C), 83.0 (4'-C), 81.2 (OC^tBu), 74.0 (2'-C), 70.2 (3'-C), 65.7 (5'-C), 50.8 (CHCH₃), 37.1 (NHCH₂), 26.8 (3C, OC^tBu), 19.1 (CHCH₃). HRMS-ESI (*m/z*): calcd for C₂₈H₃₅N₆O₉NaP [M + Na]⁺ 653.2101, found 653.2104. Found: C 53.4, H 5.6, N 13.5. Calcd for C₂₈H₃₅N₆O₉P: C 53.3, H 5.6, N 13.3%.

Phenyl (Benzoyloxy-L-alaninyl) Kinetin Riboside Phosphoramidate (13). Prepared as described for compound **11** using **2** (250 mg, 0.72 mmol), NMI (0.29 mL, 3.6 mmol), and **8** (765 mg, 2.16 mmol). The crude product was purified via flash column chromatography to yield the final product as a white solid (60 mg, 13%) (eluent 3:97 to 5:95 MeOH/CH₂Cl₂). ³¹P NMR (120 MHz, MeOD) δ 3.89, 3.64; ¹H NMR (400 MHz, MeOD) δ 8.26 (1H, s,

ArN-CH), 8.20, 8.17 (1H, 2 s, ArN-CH), 7.41 (1H, d, J = 1.8, CH₂ArO-H), 7.32–7.24 (7H, m, Ph-H), 7.21–7.06 (3H, m, Ph-H), 6.32 (1H, dd, J = 3.3, 1.9 Hz, CH₂ArO-H), 6.29 (1H, d, J = 3.2 Hz, CH₂ArO-H), 6.03 (1H, t, J = 4.9 Hz, 1'-H), 5.18–4.98 (2H, 2 m, CH₂Ph), 4.77 (2H, br s, NHCH₂), 4.67–4.57 (1H, m, 2'-H), 4.43–4.33 (3H, m, 3'-H/4'-H/5'-H), 4.33–4.20 (1H, m, 5'-H), 4.02–3.85 (1H, m, CHCH₃), 1.25 (3H, dd, J = 19.4, 7.0 Hz, CHCH₃); ¹³C NMR (100 MHz, MeOD) δ 174.8 (COOCH₂Ph), 155.8 (ArN-C), 153.9 (ArN-CH), 152.0 (Ph-C), 150.2 (ArN-C), 143.3 (ArO-CH), 140.6 (ArN-CH), 139.0 (Ph-CH), 137.1 (Ph-C), 130.7, 129.2, 128.8, 126.2, 121.9, 121.3 (Ph-CH), 121.0 (ArN-C), 111.4, 108.2 (ArO-CH), 89.9 (1'-CH), 84.3 (4'-C), 75.4 (2'-CH), 71.4 (3'-CH), 67.7 (CH₂Ph), 67.1 (5'-C), 51.5 (CHCH₃), 38.2 (NHCH₂), 20.4 (CHCH₃). HRMS-ESI (*m/z*): calcd for C₃₁H₃₃N₆O₉NaP [M + Na]⁺ 687.1944, found 687.1942. Found: C 55.95, H 5.2, N 12.6. Calcd for C₃₁H₃₃N₆O₉P: C 56.0, H 5.0, N 12.65%.

Phenyl (Isopropoxy-L-alaninyl) Kinetin Riboside Phosphoramidate (14). Prepared as described for compound **11** using **2** (250 mg, 0.72 mmol), NMI (0.29 mL, 3.60 mmol), and **9** (660 mg, 2.16 mmol). The crude product was purified via flash column chromatography to yield the final product as a white solid (185 mg, 42%) (eluent 3:97 to 5:95 MeOH/CH₂Cl₂). ³¹P NMR (120 MHz, CDCl₃) δ 3.02, 2.86; ¹H NMR (400 MHz, CDCl₃) δ 8.27 (1H, s, ArN-CH), 7.98, 7.94 (1H, 2 s, ArN-CH), 7.30 (1H, dd, J = 2.5, 1.4 Hz, CH₂ArO-H), 7.15 (2H, t, J = 7.7 Hz, Ph-H), 7.07 (2H, d, J = 7.7 Hz, Ph-H), 7.00 (1H, m, Ph-H), 6.74 (1H, br s, NHCH₂ArO), 6.25 (2H, t, J = 1.7 Hz, CH₂ArO-H), 5.98 (1H, t, J = 4.4 Hz, 1'-H), 5.38 (1H, br s, O-H), 4.96–4.85 (1H, m, OCHⁱPr), 4.78 (2H, br s, NHCH₂ArO), 4.57–4.25 (6H, m, NHCHCH₃, 2'-H, 3'-H, 4-H, 5'-H₂), 3.94–3.81 (1H, m, NHCHCH₃), 1.24 (3H, t, J = 7.2 Hz, NHCHCH₃), 1.19–1.05 (6H, m, OCHⁱPr); ¹³C NMR (100 MHz, CDCl₃) δ 172.9 (CO), 154.0 (ArNC), 152.6 (ArNC-H), 151.4 (ArO-C), 150.2 (Ph-C), 148.5 (ArNC), 142.0 (ArO-CH), 138.6 (ArNC-H), 129.4 (Ph-CH), 124.7 (Ph-CH), 119.8 (Ph-CH), 119.6 (ArNC), 110.6 (ArO-CH), 107.3 (ArO-CH), 88.9 (1'-C), 83.1 (4'-C), 74.5 (2'-C), 70.4 (3'-C) 68.9 (OCHⁱPr), 65.8 (5'-C), 50.0 (NHCHCH₃), 37.2 (NHCH₂ArO), 21.4 (OCHⁱPr), 20.5 (NHCHCH₃). HRMS-ESI (*m/z*): calcd for C₂₇H₃₄N₆O₉P [M + H]⁺ 617.2125, found 617.2144. HPLC CH₃CN/H₂O 0:100 to 100:0 in 30 min, λ = 254 nm, t_R = 16.51, 16.69 min.

Cathepsin A Assay. Procedure was adapted from Mehellou et al.¹⁶ ProTide **14** (5.0 mg) was dissolved in acetone-*d*₆ (0.15 mL), followed by addition of Trizma buffer (0.30 mL, pH 7.4). After recording a control ³¹P NMR spectrum containing ProTide in acetone-*d*₆ and buffer, defrosted cathepsin A (0.1 mg dissolved in 0.15 mL of Trizma buffer) was added to the mixture. A ³¹P NMR was then run immediately after the addition and then at even time intervals over 11 h. The sample was then analyzed by ³¹P NMR after 24 and 48 h. All ³¹P NMR spectra recorded at 22 °C (±1).

Serum Stability. Procedure was adapted from Slusarczyk et al.²⁵ ProTide **14** (5.0 mg) was dissolved in DMSO-*d*₆ (0.10 mL) and D₂O (0.15 mL). All ³¹P NMR spectra were recorded at 37 °C. Two control spectra were recorded, one containing ProTide **14** (5.0 mg) in DMSO-*d*₆ (0.10 mL) and D₂O (0.15 mL) and the other containing defrosted human serum (0.3 mL), DMSO-*d*₆ (0.10 mL), and D₂O (0.15 mL). Following this, a previously defrosted serum (human or mouse) (0.30 mL) was added to the NMR tube and a spectrum immediately run. Spectra were recorded at 30 min after the addition and then at even time intervals over 11 h.

Acid Stability. Procedure was adapted from Slusarczyk et al.²⁵ To ProTide **12** (5 mg) in methanol-*d*₄ (0.25 mL) was added acidic buffer, pH 1 (prepared from equal parts of 0.2 M HCl and 0.2 M KCl). The sample was then subjected to ³¹P NMR experiments at 37 °C, and the spectra were recorded every 20 min over 12 h.

Docking Studies. PC Windows 7 with Intel Core i7-4790/3.6GHz microprocessor, 16 GB RAM, and 64 bit operating system was used to execute the computational studies. Docking was performed applying the molecular modeling modules, namely, Omega2, FRED, and VIDA provided by OpenEye Scientific Software (<http://www.eyesopen.com>). The three-dimensional crystal structure of the cocrystallized

AMP with the human HINT1 was retrieved from the Protein Data Bank (PDB code 1KPF),²⁶ and the active site was subsequently identified on the basis of the bound ligand. Multiple conformers for metabolite 17 were generated by Omega2 using the default settings.²⁷ FRED (fast rigid exhaustive docking) implements a rigid docking approach to fit these conformers into the predefined binding site and rank the poses by scoring functions.^{28,29} The VIDA module was then used to visualize and inspect the docked poses within the receptor's active site and to identify the main interacting residues.

Cell Studies. Flp-In T-Rex HEK293 cells stably expressing PINK1-FLAG wild-type were generated previously.²³ Cells were maintained in DMEM (Dulbecco's modified Eagle medium) supplemented with 10% (v/v) fetal bovine serum, 2 mM L-glutamine, 100 U/mL penicillin, and 0.1 mg/mL streptomycin, plus 15 μ g/mL blasticidin and 100 μ g/mL hygromycin at 37 °C under a 5% CO₂ atmosphere. On day 0, cells were seeded in DMEM. One day 1, cells were transiently transfected with wild type or S65A Parkin using polyethylenimine (Polysciences) according to the manufacturer's instruction. One day 2, PINK1-FLAG overexpression was induced by adding 0.1 μ g/mL doxycycline in DMEM for 24 h before treating cells with compounds or mitochondrial uncoupler, CCCP, as indicated in the figure legends. All compounds were dissolved in DMSO.

Sample Preparation and Immunoblotting. This was carried out as we reported previously.²³ *Lysis Buffer Used:* 50 mM Tris-HCl (pH 7.5), 1 mM EDTA, 1 mM EGTA, 1% (w/v) Triton, 1 mM sodium orthovanadate, 10 mM sodium glycerophosphate, 50 mM sodium fluoride, 10 mM sodium pyrophosphate, 0.25 M sucrose, 0.1% (v/v) 2-mercaptoethanol, 1 mM benzamide, 0.1 mM PMSF, and protease inhibitor cocktail (Roche). *Antibodies Used:* Mouse monoclonal anti-PINK1 antibody (human PINK1 residues 125–539) was raised by Dundee Cell Products, anti-vinculin and anti-GAPDH antibodies were obtained from Cell Signaling Technology, anti-Parkin phospho-serine 65 rabbit monoclonal antibody was raised by Epitomics in collaboration with the Michael J. Fox Foundation for Research, and anti-Parkin mouse monoclonal antibody was obtained from Santa Cruz.

■ ASSOCIATED CONTENT

■ Supporting Information

The Supporting Information is available free of charge on the ACS Publications website at DOI: 10.1021/acs.jmedchem.6b01897.

Molecular formula strings (CSV)

¹H NMR and ¹³C NMR spectra, HPLC data, and the mass spectra of the cathepsin A sample (PDF)

■ AUTHOR INFORMATION

Corresponding Authors

*M.M.K.M.: phone, +44(0)1382388377; e-mail, m.muqit@dundee.ac.uk.

*Y.M.: phone, +44(0)2920875821; e-mail, MehellouY1@cardiff.ac.uk.

ORCID

Youcef Mehellou: [0000-0001-5720-8513](https://orcid.org/0000-0001-5720-8513)

Author Contributions

#L.O. and Y.-C.L. contributed equally. The manuscript was written by Y.M., and all the authors provided comments and gave approval to the final version of the manuscript.

Notes

The authors declare no competing financial interest.

■ ACKNOWLEDGMENTS

M.M.K.M. is funded by a Wellcome Trust Senior Research Fellowship in Clinical Science (Grant 101022/Z/13/Z), the Medical Research Council; Parkinson's UK; the Michael J. Fox

Foundation; J. Macdonald Menzies Charitable Trust Prize Studentship, Biotechnology and Biological Sciences Research Council; and the EMBO Young Investigator Programme.

■ ABBREVIATIONS USED

CCCP, carbonyl cyanide *m*-chlorophenylhydrazine; DCM, dichloromethane; Et₂O, diethyl ether; Et₃N, triethylamine; EtOH, ethanol; KR, kinetin riboside; NMI, *N*-methylimidazole; OMM, outer mitochondrial membrane; PD, Parkinson's disease; PINK1, PTEN-induced putative kinase 1; POCl₃, phosphorus oxychloride; PTEN, phosphatase and tensin homolog; rt, room temperature; ⁴BuMgCl, *tert*-butyl magnesium chloride; TEA, triethylamine; Trizma, tris-(hydroxymethyl)aminomethane

■ REFERENCES

- (1) Dorsey, E. R.; Constantinescu, R.; Thompson, J. P.; Biglan, K. M.; Holloway, R. G.; Kieburtz, K.; Marshall, F. J.; Ravina, B. M.; Schifitto, G.; Siderowf, A.; Tanner, C. M. Projected number of people with Parkinson disease in the most populous nations, 2005 through 2030. *Neurology* **2007**, *68*, 384–386.
- (2) Rascol, O.; Payoux, P.; Ory, F.; Ferreira, J. J.; Brefel-Courbon, C.; Montastruc, J. L. Limitations of current Parkinson's disease therapy. *Ann. Neurol.* **2003**, *53*, S3–S12.
- (3) Valente, E. M.; Abou-Sleiman, P. M.; Caputo, V.; Muqit, M. M.; Harvey, K.; Gispert, S.; Ali, Z.; Del Turco, D.; Bentivoglio, A. R.; Healy, D. G.; Albanese, A.; Nussbaum, R.; Gonzalez-Maldonado, R.; Deller, T.; Salvi, S.; Cortelli, P.; Gilks, W. P.; Latchman, D. S.; Harvey, R. J.; Dallapiccola, B.; Auburger, G.; Wood, N. W. Hereditary early-onset Parkinson's disease caused by mutations in PINK1. *Science* **2004**, *304*, 1158–1160.
- (4) Kazlauskaite, A.; Muqit, M. M. PINK1 and Parkin- mitochondrial interplay between phosphorylation and ubiquitylation in Parkinson's disease. *FEBS J.* **2015**, *282*, 215–223.
- (5) Lucking, C. B.; Durr, A.; Bonifati, V.; Vaughan, J.; De Michele, G.; Gasser, T.; Harhangi, B. S.; Meo, G.; Deneffe, P.; Wood, N. W.; Agid, Y.; Brice, A. French Parkinson's Disease Genetics Study Group; European Consortium on Genetic Susceptibility in Parkinson's Disease. Association between early-onset Parkinson's disease and mutations in the Parkin gene. *N. Engl. J. Med.* **2000**, *342*, 1560–1567.
- (6) Pickrell, A. M.; Youle, R. J. The roles of PINK1, Parkin, and mitochondrial fidelity in Parkinson's disease. *Neuron* **2015**, *85*, 257–273.
- (7) Song, S.; Jang, S.; Park, J.; Bang, S.; Choi, S.; Kwon, K. Y.; Zhuang, X.; Kim, E.; Chung, J. Characterization of PINK1 (PTEN-induced putative kinase 1) mutations associated with Parkinson disease in mammalian cells and Drosophila. *J. Biol. Chem.* **2013**, *288*, 5660–5672.
- (8) Woodroof, H. I.; Pogson, J. H.; Begley, M.; Cantley, L. C.; Deak, M.; Campbell, D. G.; van Aalten, D. M.; Whitworth, A. J.; Alessi, D. R.; Muqit, M. M. Discovery of catalytically active orthologues of the Parkinson's disease kinase PINK1: analysis of substrate specificity and impact of mutations. *Open Biol.* **2011**, *1*, 110012.
- (9) Kim, Y.; Park, J.; Kim, S.; Song, S.; Kwon, S. K.; Lee, S. H.; Kitada, T.; Kim, J. M.; Chung, J. PINK1 controls mitochondrial localization of Parkin through direct phosphorylation. *Biochem. Biophys. Res. Commun.* **2008**, *377*, 975–980.
- (10) Hertz, N. T.; Berthet, A.; Sos, M. L.; Thorn, K. S.; Burlingame, A. L.; Nakamura, K.; Shokat, K. M. A neo-substrate that amplifies catalytic activity of Parkinson's-disease-related kinase PINK1. *Cell* **2013**, *154*, 737–747.
- (11) www.clinicaltrials.gov (accessed March 8, 2017).
- (12) Narendra, D. P.; Jin, S. M.; Tanaka, A.; Suen, D. F.; Gautier, C. A.; Shen, J.; Cookson, M. R.; Youle, R. J. PINK1 is selectively stabilized on impaired mitochondria to activate Parkin. *PLoS Biol.* **2010**, *8*, e1000298.

(13) Mehellou, Y.; Balzarini, J.; McGuigan, C. Aryloxy phosphoramidate triesters: a technology for delivering monophosphorylated nucleosides and sugars into cells. *ChemMedChem* **2009**, *4*, 1779–1791.

(14) Thornton, P. J.; Kadri, H.; Miccoli, A.; Mehellou, Y. Nucleoside phosphate and phosphonate prodrug clinical candidates. *J. Med. Chem.* **2016**, *59*, 10400–10410.

(15) Bressi, J. C.; Choe, J.; Hough, M. T.; Buckner, F. S.; Van Voorhis, W. C.; Verlinde, C. L.; Hol, W. G.; Gelb, M. H. Adenosine analogues as inhibitors of *Trypanosoma brucei* phosphoglycerate kinase: elucidation of a novel binding mode for a 2-amino-N(6)-substituted adenosine. *J. Med. Chem.* **2000**, *43*, 4135–4150.

(16) Mehellou, Y.; Valente, R.; Mottram, H.; Walsby, E.; Mills, K. L.; Balzarini, J.; McGuigan, C. Phosphoramidates of 2'-beta-D-arabinouridine (AraU) as phosphate prodrugs; design, synthesis, in vitro activity and metabolism. *Bioorg. Med. Chem.* **2010**, *18*, 2439–2446.

(17) Mehellou, Y. The ProTides boom. *ChemMedChem* **2016**, *11*, 1114–1116.

(18) Saboulard, D.; Naesens, L.; Cahard, D.; Salgado, A.; Pathirana, R.; Velazquez, S.; McGuigan, C.; De Clercq, E.; Balzarini, J. Characterization of the activation pathway of phosphoramidate triester prodrugs of stavudine and zidovudine. *Mol. Pharmacol.* **1999**, *56*, 693–704.

(19) Birkus, G.; Wang, R.; Liu, X.; Kutty, N.; MacArthur, H.; Cihlar, T.; Gibbs, C.; Swaminathan, S.; Lee, W.; McDermott, M. Cathepsin A is the major hydrolase catalyzing the intracellular hydrolysis of the antiretroviral nucleotide phosphonoamidate prodrugs GS-7340 and GS-9131. *Antimicrob. Agents Chemother.* **2007**, *51*, 543–550.

(20) Congiatu, C.; Brancale, A.; McGuigan, C. Molecular modelling studies on the binding of some protides to the putative human phosphoramidase Hint1. *Nucleosides, Nucleotides Nucleic Acids* **2007**, *26*, 1121–1124.

(21) Murakami, E.; Tolstykh, T.; Bao, H. Y.; Niu, C. R.; Steuer, H. M. M.; Bao, D. H.; Chang, W.; Espiritu, C.; Bansal, S.; Lam, A. M.; Otto, M. J.; Sofia, M. J.; Furman, P. A. Mechanism of activation of PSI-7851 and its diastereoisomer PSI-7977. *J. Biol. Chem.* **2010**, *285*, 34337–34347.

(22) Cheng, J. L.; Zhou, X.; Chou, T. F.; Ghosh, B.; Liu, B. L.; Wagner, C. R. Identification of the amino acid-AZT-phosphoramidase by affinity T7 phage display selection. *Bioorg. Med. Chem. Lett.* **2009**, *19*, 6379–6381.

(23) Kondapalli, C.; Kazlauskaitė, A.; Zhang, N.; Woodroof, H. I.; Campbell, D. G.; Gourlay, R.; Burchell, L.; Walden, H.; Macartney, T. J.; Deak, M.; Knebel, A.; Alessi, D. R.; Muqit, M. M. PINK1 is activated by mitochondrial membrane potential depolarization and stimulates Parkin E3 ligase activity by phosphorylating serine 65. *Open Biol.* **2012**, *2*, 120080.

(24) Stein, D. S.; Moore, K. H. P. Phosphorylation of nucleoside analog antiretrovirals: a review for clinicians. *Pharmacotherapy* **2001**, *21*, 11–34.

(25) Slusarczyk, M.; Lopez, M. H.; Balzarini, J.; Mason, M.; Jiang, W. G.; Blagden, S.; Thompson, E.; Ghazaly, E.; McGuigan, C. Application of ProTide technology to gemcitabine: a successful approach to overcome the key cancer resistance mechanisms leads to a new agent (NUC-1031) in clinical development. *J. Med. Chem.* **2014**, *57*, 1531–1542.

(26) Lima, C. D.; Klein, M. G.; Hendrickson, W. A. Structure-based analysis of catalysis and substrate definition in the HIT protein family. *Science* **1997**, *278*, 286–290.

(27) Hawkins, P. C.; Nicholls, A. Conformer generation with OMEGA: learning from the data set and the analysis of failures. *J. Chem. Inf. Model.* **2012**, *52*, 2919–2936.

(28) McGann, M. FRED pose prediction and virtual screening accuracy. *J. Chem. Inf. Model.* **2011**, *51*, 578–596.

(29) McGann, M. R.; Almond, H. R.; Nicholls, A.; Grant, J. A.; Brown, F. K. Gaussian docking functions. *Biopolymers* **2003**, *68*, 76–90.